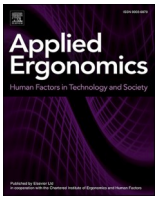
Applied Ergonomics 140 (2027) 104915



Contents lists available at ScienceDirect

Applied Ergonomics

journal homepage: www.elsevier.com/locate/apergo



Heart rate variability as a physiological marker of motion sickness in real-world driving conditions

Seonghyeon Kim [a,b,*], Cheong-Un Kim [c], Jaesik Yang [a], Chang-Hwan Im [c,d], M. Ercan Altinsoy [b]

[a] Research and Development Division, Hyundai Motor Company, Hwaseong-si, Gyeonggi-do, South Korea
[b] Chair of Acoustics and Haptics, Institute of Acoustics and Speech Communication, Technische Universität Dresden, Dresden, Germany
[c] Department of Electronic Engineering, Hanyang University, Seoul, South Korea
[d] Department of Biomedical Engineering, Hanyang University, Seoul, South Korea

ARTICLE INFO

Keywords:
Motion sickness
Electric vehicle
Autonomous vehicle
Electrocardiogram
Heart rate variability

ABSTRACT

This study investigated the utility of heart rate variability (HRV) metrics derived from electrocardiogram (ECG) signals for assessing motion sickness (MS) during real-world driving. While motion sickness is commonly evaluated through subjective reports or multimodal physiological measurements, previous studies have predominantly relied on simulator-based experiments or multimodal physiological sensing, which limit ecological validity and practical deployment in everyday vehicles. In this study, twenty-four female participants were exposed to systematically varied acceleration and deceleration profiles across 13 predefined driving conditions in an electric vehicle. Motion sickness symptoms were measured using the Misery Scale (MISC), and ECG data were segmented into 120-s epochs to extract heart rate, the low-frequency to high-frequency (LF/HF) ratio, and pNN50 (the percentage of successive normal-to-normal intervals differing by more than 50 ms). Using a threshold corresponding to symptom onset (MISC of 2 or above), pNN50 was significantly lower in the high-MS group than in the low-MS group (16.5% versus 24.6%, $p < 0.001$, Cohen's $d = -0.53$), indicating reduced parasympathetic (vagal) modulation in the presence of motion sickness symptoms. Heart rate did not differ significantly between groups, and the LF/HF ratio showed a statistically significant but negligible difference. Mean pNN50 values did not, however, decline monotonically across individual MISC scores, indicating that the metric distinguishes the presence of symptoms rather than grading their severity. These findings suggest that pNN50 is the most sensitive of the examined HRV indices and may reflect individual differences in susceptibility to motion sickness. The study demonstrates that motion sickness can be assessed using a single, widely accessible physiological signal such as ECG, providing a foundation for future wearable and in-vehicle motion sickness monitoring systems.

1. Introduction

Motion sickness is most commonly explained by the prevailing sensory-conflict theory, which attributes it to conflicts among visual, vestibular, and somatosensory inputs, although this framework does not account for all aspects of the condition. It is commonly experienced across various modes of transportation, including cars, ships, and airplanes. It induces symptoms such as nausea, dizziness, headache, and discomfort, significantly affecting individuals' productivity and overall travel experience (Bos et al., 2005, 2022; Irmak et al., 2021). In automotive environments, the mismatch between vehicle motion and passengers' bodily perceptions is a major contributing factor to motion sickness, and such conflicts are particularly pronounced among passengers engaged in non-driving-related tasks (NDRTs), such as reading or watching screens (Diels and Bos, 2016). Motion sickness is expected to become a greater challenge in autonomous vehicles compared to conventional vehicles (Sivak and Schoettle, 2015). This is because the primary factors that contribute to motion sickness, including sensory conflicts between vestibular and visual inputs, a reduced ability to predict the direction of movement, and a lack of control over motion, are amplified in self-driving environments. In autonomous vehicles, passengers transition from active drivers to entirely passive occupants. This

* Corresponding author. Chair of Acoustics and Haptics, Institute of Acoustics and Speech Communication, Technische Universität Dresden, Dresden, Germany.
E-mail addresses: seonghyeon.kim@hyundai.com, seonghyeon.kim@tu.dresden.de (S. Kim).

https://doi.org/10.1016/j.apergo.2026.104915
Received 7 May 2025; Received in revised form 25 July 2026; Accepted 13 October 2026
Available online 16 October 2026
0003-6870/© 2026 The Author(s). Published by Elsevier Ltd. This is an open access article under the CC BY license (http://creativecommons.org/licenses/by/4.0/).
Open access funding enabled and organized by Projekt DEAL.

shift enables them to engage in non-driving activities, such as reading or screen use, which, as highlighted by several studies, significantly increases the likelihood of motion sickness.

Motion sickness is not just a discomforting symptom but a complex physiological phenomenon involving interactions within the nervous and autonomic nervous systems. Stimulation of the vestibular system is closely linked to the processing of sensory signals in the brain, particularly in the vestibular cortex and midbrain, leading to the development of motion sickness symptoms. This process primarily arises from conflicts between visual information and sensory signals detected by the vestibular system, occurring when the brain's neural networks fail to maintain a balance between prior experiences and new stimuli (Yates et al., 1998). Furthermore, motion sickness disrupts autonomic nervous system balance, triggering a range of physiological responses, including nausea, increased heart rate, changes in blood pressure, excessive sweating, and suppression of gastrointestinal function (Muth, 2006; Murdin et al., 2011). These physiological changes may serve as important indicators of motion sickness severity and provide useful metrics for evaluating its physical and mental effects (Leung and Hon, 2019).

1.1. Physiological signals in motion sickness assessment

Numerous studies have reported the use of physiological signals to evaluate and analyze motion sickness (Koohestani et al., 2019; Hu et al., 1999). Various biosignals, such as electroencephalography (EEG) (Yu et al., 2010; Chen et al., 2010; Chuang et al., 2016), electrocardiography (ECG) (Holmes and Griffin, 2001), galvanic skin response (GSR) (Irmak et al., 2021), electrooculogram (EOG) (Cheung et al., 2004; Dennison et al., 2016), blood pressure, and body temperature (Graybiel and Lackner, 1980), have been employed to understand the physiological responses associated with motion sickness. EEG has been widely used to study neural activity changes in specific brain regions during motion sickness episodes. Previous studies have shown that individuals susceptible to motion sickness exhibit significant alterations in neural synchronization and phase connectivity when exposed to motion-inducing stimuli (Wei et al., 2019). More recently, Ren et al. (2024) demonstrated that EEG can effectively capture neural correlates of motion sickness by analyzing power fluctuations in specific frequency bands. Specifically, their findings indicated significant differences in the theta (4–8 Hz) and alpha (8–13 Hz) bands during motion sickness episodes, with theta band power increasing and alpha band power showing region-dependent variations. In another study, Bang et al. (2023) utilized dry EEG data collected in a real-world driving environment to predict motion sickness. Using a normalized sample covariance matrix-based feature representation method combined with convolutional neural networks for classification, their approach achieved an average accuracy of 89.05% (±5.76%) across four experimental sessions. Although EEG is considered one of the most accurate methods for assessing motion sickness, it is sensitive to artifacts caused by body movements and presents practical challenges due to the high cost of equipment and lengthy setup times. As a result, many studies have explored the use of alternative biosignals, such as GSR and ECG, for motion sickness evaluation. Previous studies utilizing optokinetic drums and virtual environments have reported that skin conductivity significantly changes during the onset of motion sickness (Hu et al., 1991; Kim et al., 2005). In particular, GSR has been widely used to measure autonomic nervous system responses to motion sickness, with both tonic and phasic components showing significant increases at higher sickness levels (Koohestani et al., 2019). Notably, tonic GSR rose by 42.5%, and phasic GSR increased by 90% at high levels on the Misery Scale (MISC) (Bos et al., 2005), indicating its strong correlation with motion sickness severity (Irmak et al., 2021).

1.2. Heart rate variability and autonomic responses

This study focuses on evaluating the relationship between ECG signals and motion sickness, with a particular emphasis on heart rate variability (HRV) metrics as indicators of autonomic nervous system activity. Given that ECG can be conveniently measured using wearable devices such as smartwatches, rings, and other portable technologies (Georgiou et al., 2018; Wang et al., 2019; Meng et al., 2021), it could serve as a promising and accessible method for detecting motion sickness in real-world scenarios. HRV has been extensively studied for its ability to reflect changes in the balance between sympathetic and parasympathetic activity during motion sickness episodes. Metrics such as low frequency (LF) power, high frequency (HF) power, and the LF/HF ratio are widely used to assess autonomic responses to physiological and psychological stressors, including motion sickness. According to Lin et al. (2011), motion sickness typically enhances sympathetic dominance, as indicated by increased LF power and LF/HF ratios, while simultaneously reducing parasympathetic activity, which is reflected by decreased HF power. However, in contrast, Naqvi et al. (Naqvi et al. (2013) reported that HRV metrics did not consistently correlate with the severity of motion sickness. Furthermore, Ohyama et al. (2007) conducted a frequency-domain analysis of HRV during visually induced motion sickness (VIMS) in a virtual reality environment. Their findings showed an increase in LF power but no significant change in HF power. These results suggest that the relationship between HRV and motion sickness may depend on experimental conditions, such as the type of motion stimulus, as well as individual variability. Moreover, most studies have focused on motion sickness induced in controlled environments, such as virtual reality or augmented reality (Koohestani et al., 2019). The mechanisms responsible for visually induced motion sickness (VIMS) and motion-induced sickness, though resulting in similar symptoms, differ significantly. VIMS is primarily attributed to conflicts between visual and vestibular inputs, commonly observed in virtual reality environments or during exposure to 3D visuals, where visual stimuli play a dominant role. In contrast, motion-induced sickness arises from discrepancies among vestibular, somatosensory, and visual signals, typically triggered by unpredictable or uncontrollable physical motion, such as that experienced in vehicles or on ships. While VIMS is predominantly influenced by visual stimuli, motion-induced sickness is more closely associated with conflicts involving vestibular and somatosensory systems. Consequently, findings from VIMS studies are often challenging to generalize to real-world scenarios, such as car sickness, where motion sickness is influenced by complex and dynamic environmental factors specific to actual driving conditions.

To the best of our knowledge, studies investigating the relationship between ECG measurements and motion-induced sickness are scarce. Shodipe et al. (Shodipe and Allison, 2023) investigated the relationship between car sickness and physiological measures such as electrocardiogram (ECG), electrodermal activity (EDA), and head movement. Their findings indicated that head movement had the strongest correlation with car sickness, while heart rate and skin conductance demonstrated moderate correlations. However, a limitation of their study is that it was conducted in a motion-based simulator rather than in real-world driving conditions, since the symptoms experienced in motion-based simulators do not fully replicate those occurring in actual driving environments (Talsma et al., 2023). Meanwhile. Irmak et al. (2021) evaluated motion sickness under real-world driving conditions and observed a gradual decrease in the LF/HF ratio during motion sickness episodes. They noted, however, that the LF/HF ratio alone may not serve as a reliable and consistent indicator of motion sickness. To further improve the application of ECG in motion sickness study, they recommended exploring the relationship between other HRV metrics, such as root mean square of successive differences (RMSSD) and the percentage of successive normal-to-normal intervals differing by more than 50 ms (pNN50) (Shaffer and Ginsberg, 2017), and the severity of motion sickness. Karjanto et al. (2022) presented a study investigating

the use of HRV metrics to evaluate motion sickness experienced while reading in fully automated driving conditions. HRV metrics such as heart rate, RMSSD, and HF components were analyzed to assess parasympathetic nervous system activity. Heart rate increased during the initial stages of driving and gradually decreased in later stages, consistent with a mild motion sickness response. Meanwhile, RMSSD, reflecting parasympathetic activity, showed an increase during the driving stages, possibly indicating a relaxation or sopite-related syndrome rather than a typical motion sickness pattern. HF components fluctuated across conditions without demonstrating consistent trends. While the study provides meaningful insights, the results showed that participants experienced mild motion sickness across all experimental conditions, but no statistically significant differences in HRV metrics were observed. Notably, a 5-min analysis window was used for HRV measurements, which may be insufficient to capture dynamic changes in heart rate over shorter time periods. Therefore, HRV analyses using shorter epochs, while still long enough to resolve the frequency bands of interest, are needed to better detect subtle physiological changes associated with motion sickness episodes.

1.3. The present study

The aim of this study is to quantitatively evaluate car motion sickness using ECG measurements. To achieve this, 24 female participants were recruited, and motion sickness was assessed in a real-world driving environment using an electric vehicle across 13 predefined acceleration and deceleration conditions. Unlike previous studies conducted in motion-based simulators, this study was performed under real-world driving conditions, providing a more physiologically valid assessment of motion sickness symptoms. Subjective evaluations were conducted using the MISC (Bos et al., 2005) and compared with ECG measurements to examine whether HRV metrics, and pNN50 in particular, differentiate levels of motion sickness severity, and to characterize the form of that relationship. This study introduces a novel approach to evaluating motion sickness by utilizing a single physiological signal, specifically electrocardiography (ECG), within a real-world driving environment. In contrast to previous research conducted in simulated settings or based on multimodal sensor systems, this study emphasizes the practical feasibility and ecological validity of ECG-based monitoring in naturalistic driving contexts. The structure of this paper is as follows: Section 2 outlines the experimental setup, including the methodology and equipment utilized. Section 3 presents the experimental results, while Section 4 discusses the findings, emphasizing the study's implications and potential avenues for future research. Finally, Section 5 concludes with a summary of the study's contributions.

2. Methods

2.1. Subjects

The present study recruited female participants exclusively, based on previous findings that women are more prone to motion sickness compared to men (Propper et al., 2018). All participants were Korean and were selected to enhance the reliability of motion sickness induction. Participants were recruited from the general public by public announcement through a professional research consulting agency. To identify susceptibility to motion sickness, the motion sickness susceptibility questionnaire (MSSQ, long form) was employed (Golding, 1998). Candidates were required to obtain an MSSQ raw score of 50 or higher, which lies at or above the population mean reported for this instrument (45.5) and therefore indicates at least average-to-high susceptibility; this criterion was adopted to enhance the reliability of motion sickness induction. Normal or corrected-to-normal vision was additionally required so that all participants could perform the visual non-driving-related task (video watching) under comparable conditions. Of 617 respondents who completed the questionnaire, 36 satisfied the MSSQ criterion together with the remaining eligibility requirements (female sex, age 23-40 years, and residence within commuting distance of the test site), and 24 participants were finally enrolled (age range: 23-40 years; median age: 34.0 years; standard deviation: 5.5 years). Prior to the experiment, participants were thoroughly briefed on the study's objectives and protocol. Written informed consent was obtained in accordance with the ethical guidelines outlined in the Declaration of Helsinki. Consistency in experimental conditions was ensured by instructing participants to sleep for a minimum of 6 h before the experiment and to avoid caffeine, alcohol, or medications for at least 24 h before participation. The study received ethical approval from the Institutional Review Board of Hallym University Sacred Heart Hospital, South Korea (IRB No. 2023-08-003-001).

2.2. Experimental environment

The study was carried out on public suburban roads located in Gyeonggi Province, South Korea. A 7-km circuit was designed as the test course and repeated multiple times to incorporate a variety of motion scenarios. These scenarios included longitudinal motions, such as acceleration, maintaining a constant speed, and deceleration, as well as lateral motions involving turning maneuvers, including four U-turn maneuvers per ride. Fig. 1 illustrates the test course employed in this study. Motion sickness was assessed under real-road driving conditions using an electric vehicle (EV6 23MY, Kia). To maintain consistency across trials, two professional drivers, both of whom had completed formal driver training programs, operated two identically configured test vehicles, following strictly predefined driving profiles. Both the experiment instructor and the participants were positioned in the rear seats of the vehicle. Each participant's seat was equipped with a tablet PC, allowing them to engage in a non-driving-related task (NDRT) by watching videos during the driving. Participants were prompted by the instructor every 2 min to assess their motion sickness level using the MISC and recorded their scores on a separate tablet device. Fig. 2 illustrates the interior conditions of the vehicle occupied by the participants.

Each session consisted of a single 30-min ride performed under one predefined driving condition, and each participant completed up to 13 sessions, each held on a separate day. The 13 conditions differed in their longitudinal motion profiles, comprising four acceleration profiles (peak longitudinal acceleration 0.2-0.3 g; jerk 0.5-1.5 g/s) and nine deceleration profiles (target deceleration −0.1 to −0.2 g; jerk −0.67 to −0.07 g/s), so that every participant experienced the same circuit under a range of motion stimuli across sessions in a within-subject design. To reproduce these profiles consistently rather than relying on driver skill alone, the vehicle's longitudinal control was modified to track the predefined targets: in the acceleration conditions, depressing the accelerator pedal commanded the vehicle control unit (VCU) to follow the prescribed target acceleration, and in the deceleration conditions, releasing the accelerator pedal (tip-out) commanded it to follow the prescribed target deceleration. The two professional drivers therefore initiated each maneuver, while the controller regulated the acceleration and deceleration to the specified profile. Table 1 summarizes the driving conditions, and Figs. 3 and 4 show representative vehicle motion data recorded during one acceleration condition and one deceleration condition, respectively. To standardize the visual environment across participants and to induce motion sickness reliably, black curtains were installed between the front and rear rows, as well as on the side windows; removing the external visual reference is a well-established provocative manipulation, and its implications for ecological validity are considered in Section 4.2.

2.3. ECG data collection

ECG data were continuously collected during the driving sessions to assess participants' physiological responses to motion sickness. ECG



Fig. 1. Test course location and route in Gyeonggi Province, South Korea, used for motion sickness evaluation under real-road driving conditions. The map and street view illustrate the 7-km circuit designed for the experiment.

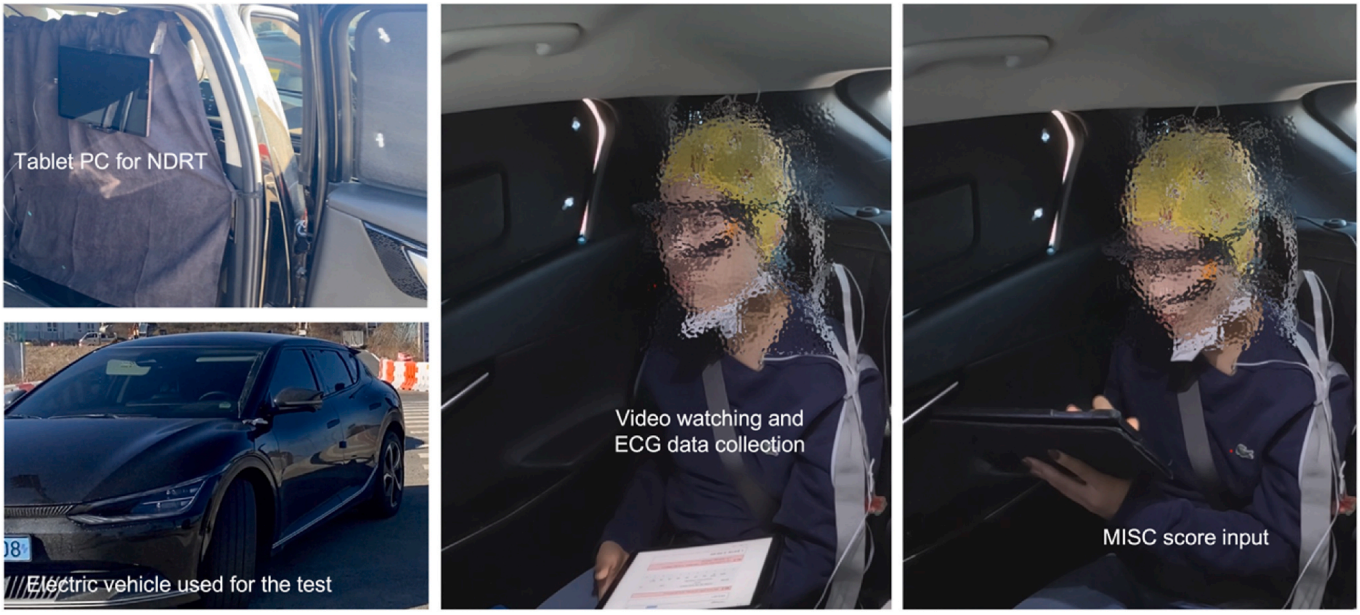


Fig. 2. Experimental setup for motion sickness evaluation in a real-road driving environment. The figure shows the electric vehicle used for the test, the tablet PC for non-driving-related tasks (NDRT), the video watching and ECG data collection process, and the MISC score input by participants during the experiment.

Table 1
Predefined longitudinal driving conditions used in the experiment.

Condition	Number of profiles	Peak/target acceleration (g)	Jerk (g/s)
Acceleration	4	0.2 to 0.3	0.5 to 1.5
Deceleration	9	−0.1 to −0.2	−0.67 to −0.07

electrodes were placed on the participants' clavicles to ensure reliable signal acquisition. Data were recorded at a sampling rate of 2048 Hz using the BioSemi ActiveTwo system (Biosemi, Amsterdam, The Netherlands). The recordings were segmented based on trigger values marking the start and end points and were downsampled to 512 Hz to optimize computational efficiency. To standardize the data collection process, the ECG device was calibrated for each participant for 1 min prior to the driving session. Participants were instructed to minimize excessive movements during the experiment to reduce potential artifacts. The collected data were processed to eliminate noise and artifacts through the application of a 1-40 Hz Butterworth band-pass filter applied using zero-phase filtfilt, ensuring high-quality signals for subsequent analysis. Major HRV metrics, including heart rate, the LF/HF ratio, and pNN50, were extracted to evaluate autonomic nervous system activity during motion sickness episodes. For MISC evaluation, HRV metrics were computed over 120-s epochs, each aligned one-to-one with the corresponding 2-min MISC rating interval. A 120-s window was selected because frequency-domain HRV requires the epoch to resolve the low-frequency band (0.04-0.15 Hz): a 30-s window spans only about 1.2 cycles of the slowest low-frequency component, whereas a 120-s window spans approximately 4.8 cycles. Results obtained with 30-s

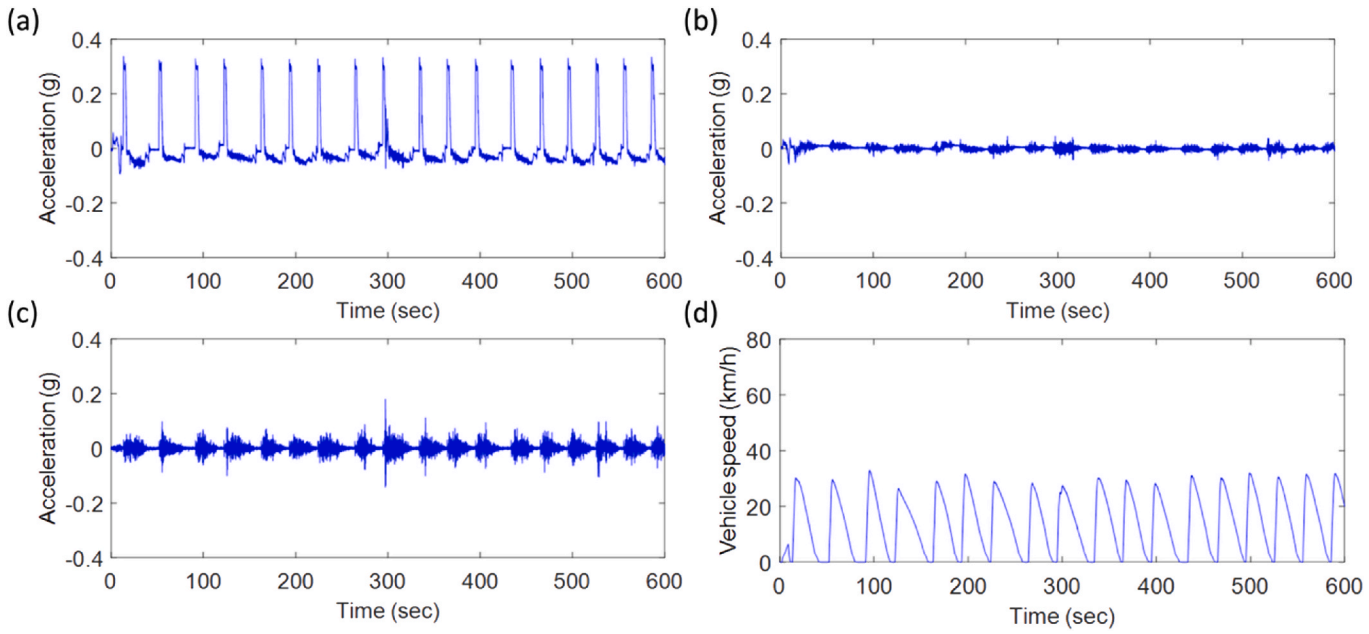


Fig. 3. Representative vehicle motion data recorded during one acceleration condition, showing longitudinal, lateral and vertical acceleration together with vehicle speed.

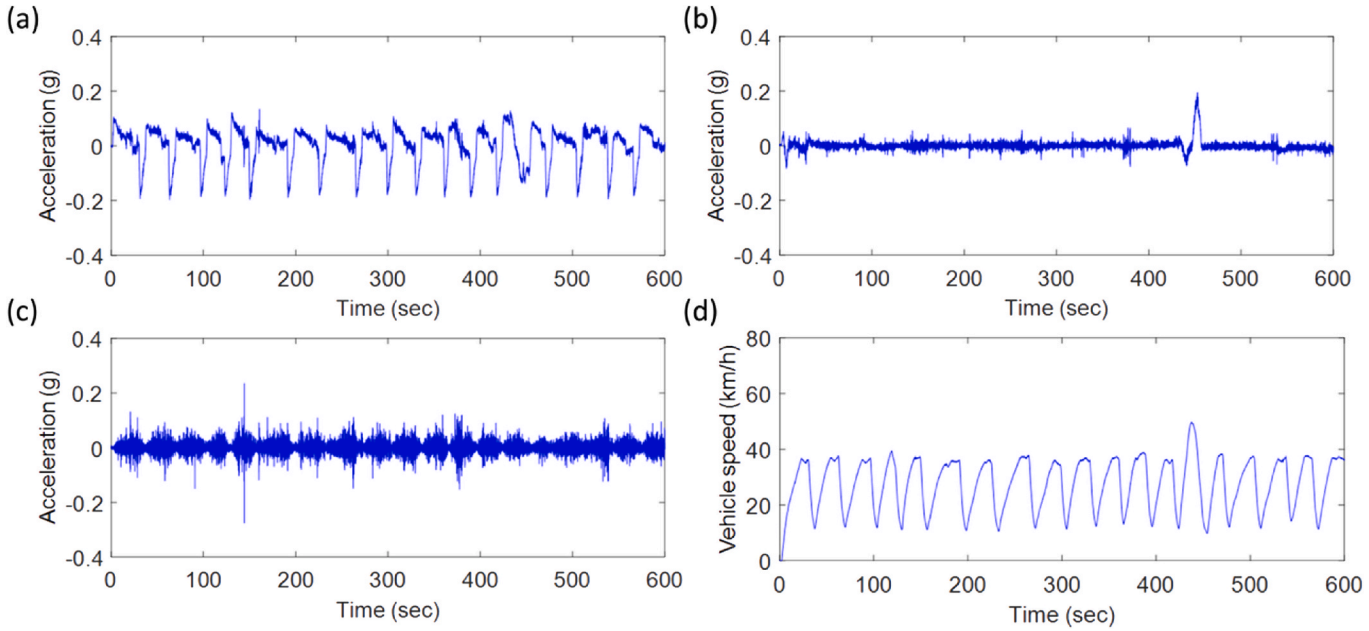


Fig. 4. Representative vehicle motion data recorded during one deceleration condition, showing longitudinal, lateral and vertical acceleration together with vehicle speed.

epochs are reported as a sensitivity analysis in Section 3.4. The ECG data were synchronized with MISC scores, recorded every 2 min, enabling detailed correlation analyses between physiological responses and subjective motion sickness severity. Fig. 5 illustrates the R-peak detection from the measured ECG data, with identified peaks marked by red circles, showing signal characteristics over a 30-s interval. R-peaks were identified using a custom amplitude-threshold and local-maximum detector. In a subset of epochs the clavicular electrode placement produced beats in which the T-wave amplitude equalled or exceeded that of the QRS complex; because an amplitude-based detector may then mistake the T-wave for the R-peak and generate spurious RR intervals that would distort the HRV metrics, and pNN50 in particular, such epochs were excluded from further analysis.

2.4. Statistical analysis

All ECG preprocessing, R-peak detection and HRV feature extraction were performed in MATLAB R2024 (MathWorks, Natick, MA, USA) using custom scripts. Statistical analyses were carried out in Python using the SciPy, statsmodels and pandas packages. Epochs were classified a priori as low-MS or high-MS on the basis of the MISC: because scores of 0 and 1 denote no specific symptoms, whereas a score of 2 marks the first appearance of specific symptoms such as dizziness, warmth, headache, stomach awareness or sweating, epochs with a MISC

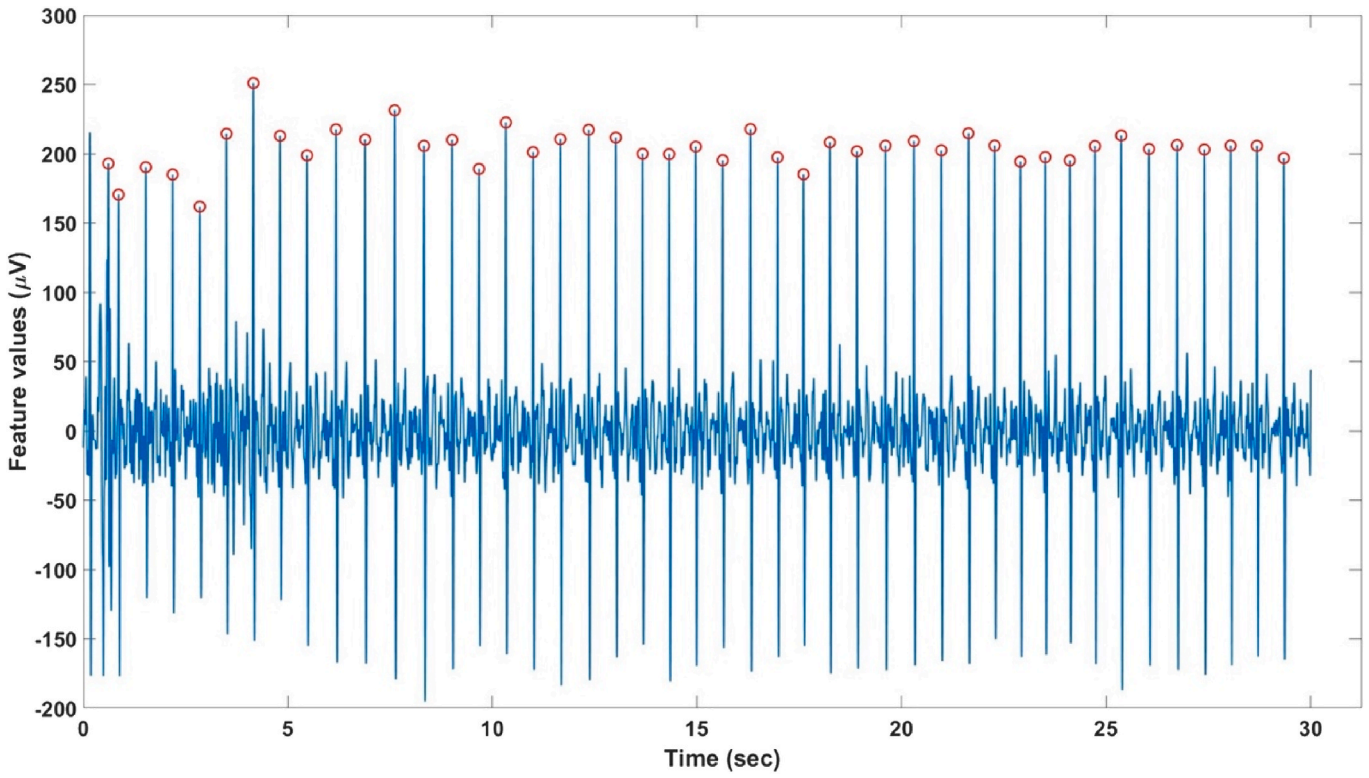


Fig. 5. R-peak detection from the measured ECG signal over a representative 30-s segment. The detected R-peaks are marked with red circles. (For interpretation of the references to color in this figure legend, the reader is referred to the Web version of this article.)

of 2 or above were assigned to the high-MS group and those below 2 to the low-MS group (Table 2). Group differences were tested with independent-samples t-tests and, because all three metrics were right-skewed (skewness 0.64 to 1.09), with Mann-Whitney U tests as a distribution-free check. Differences across the individual MISC scores were assessed with one-way analysis of variance. All tests were two-tailed with an a priori significance level of $\alpha = 0.05$. Effect sizes are reported as Cohen's *d* for pairwise comparisons (0.2, small; 0.5, medium; 0.8, large) and as η^2 for analysis of variance (0.01, small; 0.06, medium; 0.14, large). Because the MISC is an ordinal scale, Spearman rank correlations were additionally computed, and the sensitivity of the findings to the choice of dichotomization threshold was examined by repeating the group comparison for cut-offs from a MISC of 1 through a MISC of 5. Finally, linear and quadratic models were compared using a nested F-test and the Akaike information criterion in order to test for a non-linear association between pNN50 and MISC.

3. Experimental results

All participants completed the same 7-km circuit, with sessions differing only in the predefined longitudinal motion profile across the 13 driving conditions. Fig. 6 presents the MISC trajectories recorded across sessions, and the session-level trajectories of each participant are provided in Supplementary Fig. S1. Overall, the MISC scores exhibited an increasing trend over time, rising from a group mean of 1.0 at 2 min to 3.5 at 30 min, although some participants consistently reported minimal or no symptoms, indicating considerable inter-individual variability in motion sickness susceptibility. After exclusion of epochs in which R-peak detection was unreliable, 1244 valid 120-s epochs were available for analysis. MISC scores ranged from 0 to 8 (mean 2.59, standard deviation 1.74); 860 epochs (69.1%) were classified as high-MS (MISC of 2 or above) and 384 epochs (30.9%) as low-MS.

The ECG data were analyzed using three key metrics: heart rate, LF/HF ratio, and pNN50. The heart rate, representing the number of heartbeats per minute, is a fundamental measure that reflects overall cardiovascular activity. The LF/HF ratio, calculated as the ratio of LF to HF power in HRV, indicates the balance between sympathetic and parasympathetic nervous system activity, with higher values indicating a shift in sympathovagal balance toward sympathetic activity relative to parasympathetic (vagal) modulation. Lastly, pNN50 refers to the percentage of successive NN (normal-to-normal) intervals differing by more than 50 ms, serving as a measure of parasympathetic (vagal) activity and cardiac response to physiological stressors. Each of the three HRV metrics offered a complementary perspective on autonomic nervous system activity during the driving trials. Heart rate reflected overall cardiovascular load, the LF/HF ratio captured dynamic sympathovagal balance, and pNN50 provided a high-resolution indicator of parasympathetic (vagal) tone. These indices enabled a multi-dimensional evaluation of autonomic responses under motion-related stress. Although HRV metrics have been widely employed in prior studies to assess stress, fatigue, and emotional arousal, their application to motion sickness detection under naturalistic driving conditions has remained limited. Given the complex and often non-linear characteristics of autonomic responses during motion sickness, a comparative analysis of

Table 2
The Misery Scale (MISC) used to rate motion sickness severity (Bos et al., 2005).

Symptoms		MISC
No problems		0
Some discomfort but no specific symptoms		1
Dizziness, cold or warm sensation, headache, stomach or throat awareness, sweating, blurred vision, yawning, burping, tiredness, salivation, and so on, but no nausea	Vague	2
	Little	3
	Rather	4
	Severe	5
Nausea	Little	6
	Rather	7
	Severe	8
	Retching	9
Vomiting	Vomiting	10

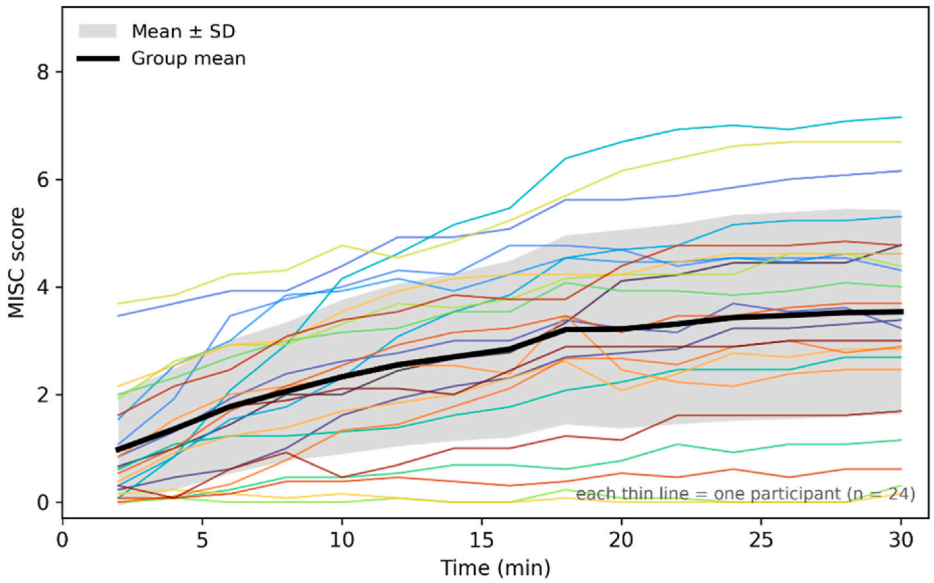


Fig. 6. Progression of motion sickness severity over time, as measured by the MISC. Each thin colored line shows the mean trajectory of one participant (n = 24; 300 sessions in total), the bold black line shows the group mean and the shaded band denotes one standard deviation across participants. MISC scores increased over the 30-min session, from a group mean of 1.0 at 2 min to 3.5 at 30 min, but inter-individual variability was considerable: some participants rose steadily to severe symptom levels whereas others reported minimal discomfort throughout. The individual session trajectories underlying each participant mean are shown in Supplementary Fig. S1.

these metrics was conducted to examine their sensitivity to symptom onset and progression. In this study, we analyzed whether ECG-derived HRV metrics could differentiate between low and high levels of subjective motion sickness, as assessed by the MISC scale. We also examined whether these metrics exhibited temporal patterns that corresponded with the severity and development of symptoms over time.

3.1. Detection of motion sickness symptoms

Epochs were classified as low-MS (MISC below 2) or high-MS (MISC of 2 or above) as described in Section 2.4. Fig. 7 illustrates the results for the three ECG metrics: (a) heart rate, (b) LF/HF ratio and (c) pNN50. Heart rate did not differ significantly between the groups, with mean values of 72.33 beats/min in the low-MS group and 73.39 beats/min in the high-MS group ($t(1242) = -1.93$, $p = 0.054$; Mann-Whitney $p = 0.841$). For the LF/HF ratio, the low-MS and high-MS groups showed mean values of 3.89 and 4.30, respectively; although this difference reached significance in the parametric test ($t(1242) = -2.20$, $p = 0.028$), the effect size was negligible (Cohen's $d = 0.13$) and the difference did not survive the distribution-free test (Mann-Whitney $p = 0.379$). By contrast, pNN50 was substantially lower in the high-MS group, with mean values of 24.60% in the low-MS group and 16.48% in the high-MS group. This difference of 8.12 percentage points was highly significant ($t(1242) = 8.63$, $p < 0.001$), corresponded to a medium effect size (Cohen's $d = -0.53$) and was equally clear without distributional assumptions (Mann-Whitney $p < 0.001$). Among the three metrics, therefore, only pNN50 showed a difference that was statistically robust, practically meaningful and independent of distributional assumptions,

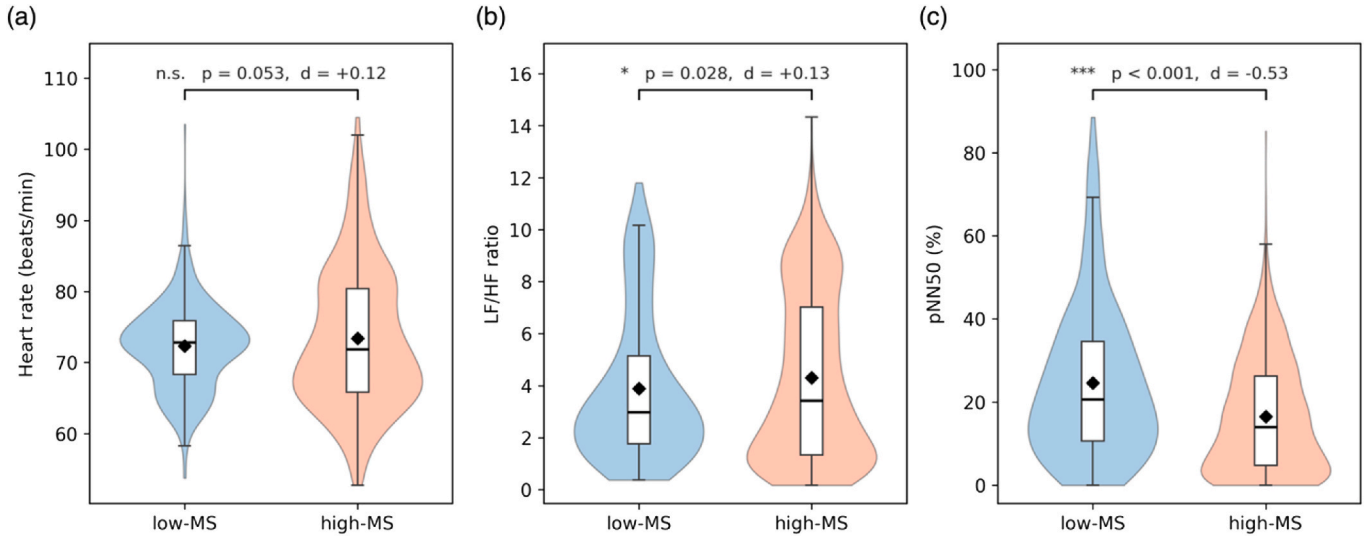


Fig. 7. Analysis of ECG metrics for low-MS (MISC below 2) and high-MS (MISC of 2 or above) groups. (a) Heart rate did not differ significantly between the groups ($p = 0.054$). (b) The LF/HF ratio was slightly higher in the high-MS group, a statistically significant but negligible difference ($p = 0.028$, $d = 0.13$). (c) pNN50 was significantly lower in the high-MS group ($p < 0.001$, $d = -0.53$), indicating reduced parasympathetic modulation.

indicating reduced parasympathetic (vagal) modulation in epochs associated with more severe motion sickness.

3.2. Physiological metrics across MISC scores

To investigate how the ECG metrics varied with motion sickness severity, the three metrics were compared across the individual MISC scores, as shown in Fig. 8. Individual scores were used rather than pooled severity categories, because pooling adjacent scores absorbs genuine between-level variation into the error term. One-way analysis of variance revealed significant differences across scores for all three metrics: heart rate ($F(8, 1235) = 13.37$, $p < 0.001$, $\eta^2 = 0.080$), pNN50 ($F(8, 1235) = 12.72$, $p < 0.001$, $\eta^2 = 0.076$) and the LF/HF ratio ($F(8, 1235) = 9.19$, $p < 0.001$, $\eta^2 = 0.056$). The variation was not, however, a graded one. Mean values fluctuated from one score to the next rather than following the severity ordering: pNN50, for example, was highest at a MISC of 1 (27.0%), fell to its lowest value at a MISC of 2 (12.8%) and rose again at a MISC of 5 (22.2%), and heart rate and the LF/HF ratio showed similarly non-monotonic patterns. The number of epochs was also small at the upper end of the scale (7 and 8 epochs at MISC scores of 7 and 8, respectively). A quadratic term fitted to pNN50 across the full MISC range was statistically significant ($F(1, 1241) = 6.69$, $p = 0.010$) but increased the explained variance by only 0.5 percentage points, and neither a linear nor a quadratic function of the MISC improved on the simple dichotomous contrast reported in Section 3.1. Taken together, these observations indicate that the HRV metrics distinguish the presence of symptoms from their absence rather than grading their severity.

3.3. Ordinal and threshold sensitivity analyses

Because the MISC is an ordinal rather than an interval scale, Spearman rank correlations were computed across the full range of scores. All three metrics were significantly correlated with the MISC: pNN50 ($\rho = -0.122$, $p < 0.001$), heart rate ($\rho = -0.106$, $p < 0.001$) and the LF/HF ratio ($\rho = +0.096$, $p < 0.001$). The negative rank correlation for pNN50 is consistent with the group comparison reported in Section 3.1. To verify that the findings did not depend on the particular dichotomization threshold, the group comparison was repeated for cut-offs ranging from a MISC of 1 to a MISC of 5 (Table 3). The reduction in pNN50 in the high-MS group was statistically significant for every cut-off from 1 to 4 (all $p < 0.001$), with effect sizes ranging from $d = -0.21$ to $d = -0.53$, and lost significance only at a cut-off of 5, where the high-MS group comprised just 112 epochs. The pNN50 finding is therefore robust to the choice of threshold. Across the same range of cut-offs, pNN50 was also the only metric whose difference retained a consistent sign and reached a medium effect size. Heart rate reversed direction, being nominally higher in the high-MS group at the lowest cut-offs and lower at cut-offs of 3 and above, while the LF/HF difference was consistent in sign but small throughout (Table 3).

3.4. Epoch-length sensitivity analysis

To assess the influence of epoch length, the analysis was repeated using 30-s epochs (1864 epochs). Rank correlations with the MISC were used throughout, for consistency with Section 3.3. Heart rate showed a stronger association at the shorter window ($\rho = -0.173$, $p < 0.001$, compared with $\rho = -0.106$, $p < 0.001$ at 120 s), whereas pNN50 lost its association ($\rho = -0.034$, $p = 0.139$, compared with $\rho = -0.122$, $p < 0.001$). The LF/HF ratio changed sign between the two epoch lengths ($\rho = +0.096$ at 120 s versus $\rho = -0.180$ at 30 s). These differences are consistent with the spectral requirements outlined in Section 2.3: a 30-s window is too short to resolve the low-frequency band reliably, and variability indices estimated over such windows are correspondingly less stable. The 120-s epoch was therefore retained for the primary analysis.

4. Discussion

This study investigated the utility of ECG metrics, including heart rate, the LF/HF ratio and pNN50, in evaluating motion sickness under real-world driving conditions. Of the three metrics, only pNN50 differentiated symptom levels with an effect size of practical relevance: pNN50 was significantly lower in the high-MS group, whereas heart rate did not differ significantly and the difference in the LF/HF ratio, although statistically significant, was negligible in magnitude.

4.1. Implications of the results

The results of this study provide meaningful insights into the use of ECG metrics for evaluating motion sickness in real-world driving conditions, particularly highlighting the potential utility of pNN50. The statistically significant reduction in pNN50 observed in the high-motion sickness (high-MS) group indicates diminished parasympathetic (vagal) modulation as symptoms become more severe, that is, a shift of sympathovagal balance toward sympathetic activity. This direction is consistent with the account of Lin et al. (2011), who reported that motion sickness enhances sympathetic dominance while reducing parasympathetic activity, and with the finding of Gianaros et al. (2003) that

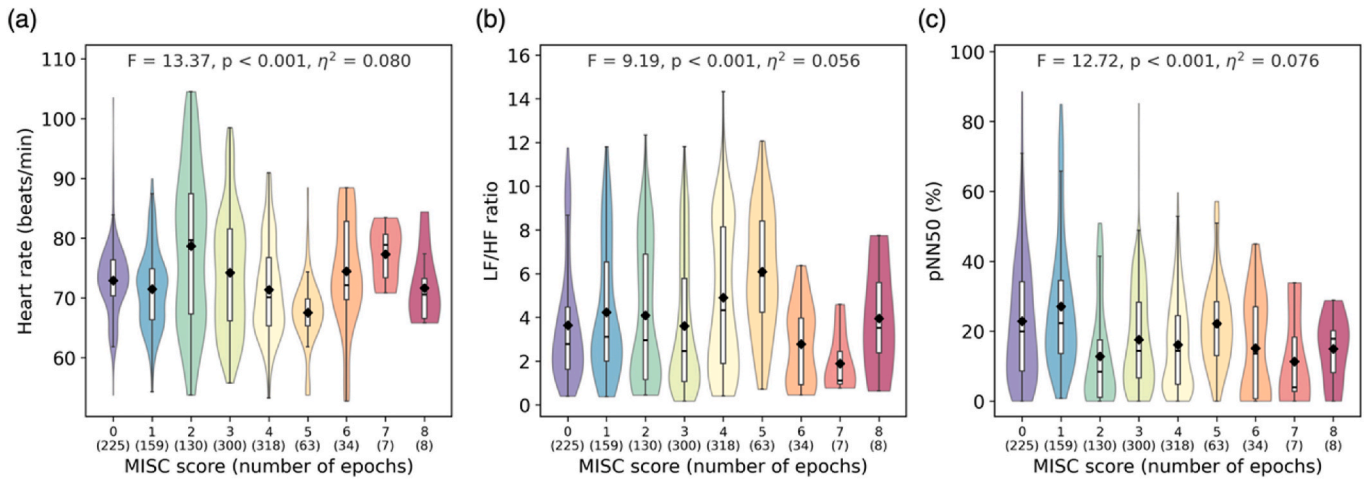


Fig. 8. ECG metrics at each MISC score. (a) Heart rate (beats/min), (b) LF/HF ratio and (c) pNN50 (%) are shown for MISC scores of 0 to 8, with the number of contributing epochs given in parentheses on the horizontal axis. Violins show the distribution, boxes the median and interquartile range, and diamonds the mean. All three metrics differed significantly across scores, but the variation was non-monotonic rather than graded, and the two highest scores are represented by few epochs.

Table 3
Sensitivity of the low-MS versus high-MS group difference to the choice of dichotomization threshold, for all three ECG metrics. Cohen's d is given with the p value of the independent-samples *t*-test in parentheses.

MISC cut-off	n (low-MS)	n (high-MS)	Heart rate	LF/HF	pNN50
≥ 1	225	1019	+0.02 (0.804)	+0.21 (0.004)	−0.30 (<0.001)
≥ 2	384	860	+0.12 (0.054)	+0.13 (0.028)	−0.53 (<0.001)
≥ 3	514	730	−0.17 (0.004)	+0.13 (0.025)	−0.29 (<0.001)
≥ 4	814	430	−0.32 (<0.001)	+0.34 (<0.001)	−0.21 (<0.001)
≥ 5	1132	112	−0.31 (0.002)	+0.18 (0.075)	−0.01 (0.919)

greater decreases in cardiac parasympathetic activity over time accompany more severe motion sickness. Doweck et al. (1997) similarly reported alterations in RR interval variability during experimentally induced motion sickness. It is also consistent with the general observation that reduced short-term heart rate variability reflects withdrawal of vagal modulation under physiological challenge (Shaffer and Ginsberg, 2017). The absence of a meaningful difference in heart rate and the very small difference in the LF/HF ratio may reflect the complexity of autonomic modulation during motion sickness. These findings echo prior research indicating that LF/HF ratios, while widely used, are not consistently reliable across different motion sickness contexts and experimental conditions (Irmak et al., 2021; Naqvi et al., 2013). The observed variability in autonomic responses underscores the need for a more nuanced interpretation of HRV metrics in motion sickness studies.

The association was, however, not a graded one. Although pNN50 clearly separated the low- and high-MS groups, mean values at the individual MISC scores varied non-monotonically and did not track symptom severity in a stepwise fashion (Fig. 8). This pattern is consistent with the substantial inter-individual variability considered below, and with the small number of epochs available at the highest symptom levels. Some authors have reported a parasympathetic rebound or compensatory vagal activation in response to sustained vestibular discomfort (Shi et al., 2025; Farmer et al., 2014); the present data neither establish nor exclude such a late-phase effect, because the epochs recorded at the most severe levels were too few to characterize it.

An important qualification concerns the level at which the present association operates. Because each participant contributed many epochs, the group difference in pNN50 reflects, to a substantial degree, differences between individuals rather than moment-to-moment changes within a given individual. The most defensible interpretation is therefore that a lower level of vagal modulation characterizes individuals who are more prone to motion sickness, so that pNN50 may serve as an indicator of individual susceptibility. Establishing whether pNN50 also tracks symptom development within a single person, which is the property required for continuous monitoring, will require designs with repeated within-participant observations and is beyond what the present data can demonstrate.

Given the feasibility of ECG sensing through wearable or seat-embedded devices, HRV, and pNN50 in particular, remains a promising candidate for passive and non-invasive assessment of motion sickness (Russell et al., 2014), and could in principle inform adaptive in-vehicle interventions such as changes in motion profiles (Siddiqi et al., 2022; Htike et al., 2022), seat vibration cues (Reuten et al., 2023; Li and Chen, 2022) or visual stabilization (Emond et al., 2024). These applications should, however, be regarded as directions for future work pending within-individual validation. It is also notable that some participants exhibited minimal or no symptoms, indicating substantial inter-individual variability (Farmer et al., 2014). Future studies should consider baseline physiological traits, motion sickness history, or adaptation effects to better understand why some individuals are more resistant to motion-induced autonomic disruption.

The present findings may also have implications for automated driving. Because our participants were seated in the rear, engaged in a visual non-driving-related task and screened from the external visual reference, their situation approximates that of a passenger in a highly automated vehicle. In such a vehicle the occupant loses both the ability to anticipate the trajectory of the vehicle and active control over it, and is more likely to engage in non-driving-related tasks; each of these factors is known to aggravate motion sickness (Diels and Bos, 2016; Sivak and Schoettle, 2015). The autonomic changes observed here might therefore be expected to be at least as pronounced, and possibly more pronounced, under automated driving than under the conditions studied here.

While pNN50 differentiated the low- and high-MS groups, it did not decline monotonically across every incremental severity level. This non-monotonic pattern, together with the considerable individual differences in autonomic responsiveness, limits the resolution with which HRV-based metrics can track symptom progression, even though they distinguish broad symptom levels.

4.2. Limitations and future works

This study has several limitations that require consideration. The relatively small sample size limits the generalizability of the findings; although 24 participants were enrolled, epochs from 17 participants satisfied the ECG quality criteria and entered the analysis. Moreover, the exclusive recruitment of female participants, selected due to their higher susceptibility to motion sickness, affects the applicability of the results to broader populations. Future studies should aim to include larger and more diverse participant groups, considering variations in sex, age, and motion sickness susceptibility, to enhance the robustness and validity of the findings. Two features of the present design were deliberately provocative and should be borne in mind when generalizing the results. Participants were seated in the rear of the vehicle and the external visual reference was screened by curtains; both manipulations were adopted to standardize the visual environment and to induce motion sickness reliably. Occupants of a front seat, who retain a forward view and can therefore anticipate the trajectory of the vehicle, would be expected to experience less severe symptoms (Griffin and Newman, 2004), since the ability to anticipate imminent motion is itself known to reduce symptom severity (Kuiper et al., 2020); the same reasoning applies to the removal of the external visual reference by the curtains, which has been shown to aggravate symptoms relative to an outside view (Bos et al., 2005). The present conditions therefore probably represent a comparatively strong provocation.

Although this study was conducted in a real-world driving environment, the controlled nature of the test route may not fully represent the diverse motion stimuli encountered in everyday driving. Factors such as urban traffic, varying road conditions, and environmental influences, including weather, were not included in this study. These uncontrolled variables could have a substantial impact on motion sickness outcomes. Future study should incorporate these factors to improve the ecological validity of the findings. A further methodological limitation concerns the structure of the data. Each participant contributed multiple epochs from multiple sessions, so the epochs are not statistically independent. The analyses reported here treat the epoch as the unit of observation, which maximizes statistical power but means that the observed group differences are influenced by variation between participants as well as by changes in symptom state within participants; as noted in Section 4.1, the association should accordingly be read primarily as an indication of

individual susceptibility. In addition, the LF/HF ratio should be interpreted with caution, because frequency-domain indices are sensitive to epoch length and to the estimation method, as the sensitivity analysis in Section 3.4 illustrates.

Furthermore, to translate these findings into real-world applications, future study should focus on the development of real-time motion sickness detection systems using ECG data. This would involve creating algorithms capable of identifying the onset of motion sickness with high accuracy. Such systems could be integrated with countermeasures, including vehicle motion control, visual stabilization, and predictive cueing systems (Kuiper et al., 2020; Reuten et al., 2023, 2024; Emond et al., 2024; Li and Chen, 2022; Siddiqi et al., 2022; Htike et al., 2022), to effectively alleviate symptoms. Additionally, evaluating these technologies in diverse real-world driving scenarios will be critical to ensure their practical implementation in commercial autonomous vehicles.

5. Conclusion

This study examined the potential of ECG metrics, including heart rate, the LF/HF ratio and pNN50, as indicators of motion sickness severity in a real-world driving environment. Among these, pNN50 was significantly lower in epochs associated with higher levels of motion sickness, with a medium effect size, indicating reduced parasympathetic modulation as symptoms became more severe. The association was not graded, however: mean values did not decline monotonically across individual MISC scores. In contrast, heart rate did not differ significantly, and the difference in the LF/HF ratio, although statistically significant, was negligible. These results reflect the complex nature of autonomic responses in real-world settings. The findings demonstrate that ECG is a feasible, non-invasive method for motion sickness evaluation, and that pNN50 in particular may index the susceptibility of an individual to motion sickness. Because each participant contributed many epochs, however, the extent to which pNN50 tracks symptom development within a single individual remains to be established. Combining ECG with other physiological signals, such as electrodermal activity or head movement, could enhance detection accuracy. In conclusion, this study contributes to the understanding of physiological measures for motion sickness evaluation and provides a basis for further studies exploring the relationship between ECG metrics and motion sickness under varied conditions.

CRediT authorship contribution statement

Seonghyeon Kim: Writing – review & editing, Writing – original draft, Visualization, Validation, Supervision, Resources, Project administration, Methodology, Investigation, Formal analysis, Data curation, Conceptualization, Software, Funding acquisition. **Cheong-Un Kim:** Writing – review & editing, Software, Methodology, Data curation, Investigation. **Jaesik Yang:** Writing – review & editing, Resources, Methodology, Investigation, Data curation, Conceptualization. **Chang-Hwan Im:** Writing – review & editing, Investigation, Conceptualization. **M. Ercan Altinsoy:** Writing – review & editing, Resources, Conceptualization.

Data availability

The data that support the findings of this study are available from the corresponding author upon reasonable request.

Funding

Open Access funding enabled and organized by Project DEAL.

Conflict of interest

The authors declare no conflict of interest.

Appendix A. Supplementary data

Supplementary data to this article can be found online at https://doi.org/10.1016/j.apergo.2026.104915.

References

Bang, J.-S., Won, D.-O., Kam, T.-E., Lee, S.-W., 2023. Motion sickness prediction based on dry EEG in real driving environment. IEEE Trans. Intell. Transport. Syst. 24 (5), 5442–5455.

Bos, J.E., Diels, C., Souman, J.L., 2022. Beyond seasickness: a motivated call for a new motion sickness standard across motion environments. Vibration 5 (4), 755–769.

Bos, J.E., MacKinnon, S.N., Patterson, A., 2005. Motion sickness symptoms in a ship motion simulator: effects of inside, outside, and no view. Aviat Space Environ. Med. 76 (12), 1111–1118.

Chen, Y.C., Duann, J.R., Chuang, S.W., Lin, C.L., Ko, L.W., Jung, T.P., et al., 2010. Spatial and temporal EEG dynamics of motion sickness. Neuroimage 49 (3), 2862–2870. https://doi.org/10.1016/j.neuroimage.2009.10.005. Epub 20091013PubMed PMID: 19833217.

Cheung, B., Hofer, K., Heskin, R., Smith, A., 2004. Physiological and behavioral responses to an exposure of pitch illusion in the simulator. Aviat Space Environ. Med. 75 (8), 657–665.

Chuang, S.-W., Chuang, C.-H., Yu, Y.-H., King, J.-T., Lin, C.-T., 2016. EEG alpha and gamma modulators mediate motion sickness-related spectral responses. Int. J. Neural Syst. 26 (2), 1650007.

Dennison, M.S., Wisti, A.Z., D'Zmura, M., 2016. Use of physiological signals to predict cybersickness. Displays 44, 42–52.

Diels, C., Bos, J.E., 2016. Self-driving carsickness. Appl. Ergon. 53, 374–382.

Doweck, I., Gordon, C.R., Shlitner, A., Spitzer, O., Gonen, A., Binah, O., et al., 1997. Alterations in R–R variability associated with experimental motion sickness. J. Auton. Nerv. Syst. 67 (1–2), 31–37.

Emond, W., Bohrmann, D., Zare, M., 2024. Will visual cues help alleviating motion sickness in automated cars? A review article. Ergonomics 67 (6), 772–800.

Farmer, A.D., Al, Omran Y., Aziz, Q., Andrews, P.L., 2014. The role of the parasympathetic nervous system in visually induced motion sickness: systematic review and meta-analysis. Exp. Brain Res. 232, 2665–2673.

Georgiou, K., Larentzakis, A.V., Khamis, N.N., Alsuhaibani, G.I., Alaska, Y.A., Giallafos, E.J., 2018. Can wearable devices accurately measure heart rate variability? A systematic review. Folia Med. 60 (1), 7–20.

Gianaros, P.J., Quigley, K.S., Muth, E.R., Levine, M.E., Vasko, J., Raymond, C., Stern, R. M., 2003. Relationship between temporal changes in cardiac parasympathetic activity and motion sickness severity. Psychophysiology 40 (1), 39–44.

Golding, J.F., 1998. Motion sickness susceptibility questionnaire revised and its relationship to other forms of sickness. Brain Res. Bull. 47 (5), 507–516.

Graybiel, A., Lackner, J.R., 1980. Evaluation of the relationship between motion sickness symptomatology and blood pressure, heart rate, and body temperature. Aviat Space Environ. Med. 51 (3), 211–214.

Griffin, M.J., Newman, M.M., 2004. Visual field effects on motion sickness in cars. Aviat Space Environ. Med. 75 (9), 739–748.

Holmes, S.R., Griffin, M.J., 2001. Correlation between heart rate and the severity of motion sickness caused by optokinetic stimulation. J. Psychophysiol. 15 (1), 35.

Htike, Z., Papaioannou, G., Siampis, E., Velenis, E., Longo, S., 2022. Fundamentals of motion planning for mitigating motion sickness in automated vehicles. IEEE Trans. Veh. Technol. 71 (3), 2375–2384.

Hu, S., Grant, W.F., Stern, R.M., Koch, K.L., 1991. Motion sickness severity and physiological correlates during repeated exposures to a rotating optokinetic drum. Aviat Space Environ. Med. 62 (4), 308–314.

Hu, S., McChesney, K.A., Player, K.A., Bahl, A.M., Buchanan, J.B., Scozzafava, J.E., 1999. Systematic investigation of physiological correlates of motion sickness induced by viewing an optokinetic rotating drum. Aviat Space Environ. Med. 70 (8), 759–765.

Irmak, T., Pool, D.M., Happee, R., 2021. Objective and subjective responses to motion sickness: the group and the individual. Exp. Brain Res. 239 (2), 515–531.

Karjanto, J.B., Yusof, N.M., Terken, J.M., Delbressine, F.L., Rauterberg, M., 2022. Level of motion sickness based on heart rate variability when reading inside a fully automated vehicle. Mechanical Engineering for Society and Industry 2 (2), 72–81.

Kim, Y.Y., Kim, H.J., Kim, E.N., Ko, H.D., Kim, H.T., 2005. Characteristic changes in the physiological components of cybersickness. Psychophysiology 42 (5), 616–625.

Koohestani, A., Nahavandi, D., Asadi, H., Kebria, P.M., Khosravi, A., Alizadehsani, R., et al., 2019. A knowledge discovery in motion sickness: a comprehensive literature review. IEEE Access 7, 85755–85770. https://doi.org/10.1109/access.2019.2922993.

Kuiper, O.X., Bos, J.E., Diels, C., Schmidt, E.A., 2020. Knowing what's coming: anticipatory audio cues can mitigate motion sickness. Appl. Ergon. 85, 103068. https://doi.org/10.1016/j.apergo.2020.103068. Epub 20200206PubMed PMID: 32174356.

Leung, A.K., Hon, K.L., 2019. Motion sickness: an overview. Drugs Context 8.

Li, D., Chen, L., 2022. Mitigating motion sickness in automated vehicles with vibration cue system. Ergonomics 65 (10), 1313–1325.

Effect of respiratory modulation on relationship between heart rate variability and motion sickness. In: Lin, C.-T., Lin, C.-L., Chiu, T.-W., Duann, J.-R., Jung, T.-P. (Eds.), 2011. 2011 Annual International Conference of the. IEEE engineering in medicine and biology society. IEEE.

Meng, L., Ge, K., Song, Y., Yang, D., Lin, Z., 2021. Long-term wearable electrocardiogram signal monitoring and analysis based on convolutional neural network. IEEE Trans. Instrum. Meas. 70, 1–11.

Murdin, L., Golding, J., Bronstein, A., 2011. Managing motion sickness. Bmj 343.

Muth, E.R., 2006. Motion and space sickness: intestinal and autonomic correlates. Auton. Neurosci. 129 (1–2), 58–66.

Naqvi, S.A.A., Badruddin, N., Malik, A.S., Hazabbah, W., Abdullah, B. (Eds.), 2013. Does 3D Produce More Symptoms of Visually Induced Motion Sickness? 2013 35th Annual International Conference of the IEEE Engineering in Medicine and Biology Society. EMBC), IEEE.

Ohyama, S., Nishiike, S., Watanabe, H., Matsuoka, K., Akizuki, H., Takeda, N., et al., 2007. Autonomic responses during motion sickness induced by virtual reality. Auris Nasus Larynx 34 (3), 303–306.

Propper, R.E., Bonato, F., Ward, L., Sumner, K., 2018. Findings of an effect of gender, but not handedness, on self-reported motion sickness propensity. Biopsychosoc. Med. 12, 1–4.

Ren, B., Ren, P., Luo, W., Xin, J., 2024. A brain network analysis model for motion sickness in electric vehicles based on EEG and fNIRS signal fusion. Sensors 24 (20), 6613.

Reuten, A., Smeets, J., Rausch, J., Martens, M., Schmidt, E., Bos, J., 2023. The (in) effectiveness of anticipatory vibrotactile cues in mitigating motion sickness. Exp. Brain Res. 241 (5), 1251–1261.

Reuten, A.J.C., Yunus, I., Bos, J.E., Martens, M.H., Smeets, J.B.J., 2024. Anticipatory cues can mitigate car sickness on the road. Transport. Res. F Traffic Psychol. Behav. 105, 196–205. https://doi.org/10.1016/j.trf.2024.07.006.

Russell, M.E.B., Hoffman, B., Stromberg, S., Carlson, C.R., 2014. Use of controlled diaphragmatic breathing for the management of motion sickness in a virtual reality environment. Appl. Psychophysiol. Biofeedback 39, 269–277.

Shaffer, F., Ginsberg, J.P., 2017. An overview of heart rate variability metrics and norms. Front. Public Health 5, 258.

Shi, L., Zhao, J., Lu, J., Cao, C., Zhang, Q., Qiu, C., et al., 2025. Effects of two kinds of vestibular function training on reducing motion sickness in college students. Front. Neurol. 16, 1433065.

Modelling the relationship between the objective measures of car sickness. In: Shodipe, O.E., Allison, R.S. (Eds.), 2023. 2023 IEEE Canadian Conference on Electrical and Computer Engineering (CCECE). IEEE.

Siddiqi, M.R., Milani, S., Jazar, R.N., Marzbani, H., 2022. Ergonomic path planning for autonomous vehicles-an investigation on the effect of transition curves on motion sickness. IEEE Trans. Intell. Transport. Syst. 23 (7), 7258–7269.

Sivak, M., Schoettle, B., 2015. Motion Sickness in self-driving Vehicles. University of Michigan, Ann Arbor, Transportation Research Institute.

Talsma, T.M.W., Hassanain, O., Happee, R., de Winkel, K.N., 2023. Validation of a moving base driving simulator for motion sickness research. Appl. Ergon. 106, 103897. https://doi.org/10.1016/j.apergo.2022.103897. Epub 20221004PubMed PMID: 36206673.

Wang, N., Zhou, J., Dai, G., Huang, J., Xie, Y., 2019. Energy-efficient intelligent ECG monitoring for wearable devices. IEEE Trans. Biomed. Circuits Syst. 13 (5), 1112–1121.

Wei, Y., Okazaki, Y.O., So, R.H., Chu, W.C., Kitajo, K., 2019. Motion sickness-susceptible participants exposed to coherent rotating dot patterns show excessive N2 amplitudes and impaired theta-band phase synchronization. Neuroimage 202, 116028.

Yates, B., Miller, A., Lucot, J., 1998. Physiological basis and pharmacology of motion sickness: an update. Brain Res. Bull. 47 (5), 395–406.

An EEG-based classification system of Passenger's motion sickness level by using feature extraction/selection technologies. In: Yu, Y.-H., Lai, P.-C., Ko, L.-W., Chuang, C.-H., Kuo, B.-C., Lin, C.-T. (Eds.), 2010. The 2010 International Joint Conference on Neural Networks (IJCNN). IEEE.